ELSEVIER

International Journal of Pharmaceutics 111 (1994) 117–125

international journal of pharmaceutics

Comparison of organic solvent-based ethylcellulose coatings on KCl crystals applied by top and bottom spraying in fluidized-bed equipment

Poul Bertelsen [a,*], Finn Norring Christensen [a], Per Holm [b], Kim Jørgensen [a]

[a] *Nycomed Drug Research, P.O. Box 1185, Helseholmen 1, DK-2650 Hvidovre, Denmark*
[b] *The Royal Danish School of Pharmacy, DK-2100 Copenhagen Ø, Denmark*

Received 12 January 1994; modified version received 18 March 1994; accepted 24 March 1994

Abstract

Differences between the efficiency of organic solvent-based membranes applied by countercurrent coating and by Wurster-based, concurrent coating were examined by coating KCl crystals with an ethylcellulose-based membrane. The dissolution from crystals coated by the concurrent process was a factor 2.6–2.8 slower than that achieved by the countercurrent process as assessed at the time for dissolution of 63.2%. The factor was shown to be similar on both the laboratory and production scales. The cause of this higher efficiency was examined. The coated crystals were examined by sieve analysis, by measuring the specific surface area, the film thickness, the amount of coating dry matter applied, by scanning electron microscopy of surfaces and cross-sections, and by determining the porosity of the membranes. It was shown that only the membrane porosity can explain the differences in coating efficiency.

Keywords: Concurrent coating; Countercurrent coating; Dissolution testing; Film thickness; Film dry matter quantity; Scanning electron microscopy; Film porosity

1. Introduction

Controlled-release coating of pellets or crystals is often carried out in fluid-bed equipment. The two main principles are countercurrent (top spray) coating and concurrent (bottom spray) coating (Jones, 1988). Differences in the efficiency of organic solvent-based coating applied by top spraying and by Wurster-based bottom spraying are generally recognized. Mehta et al. (1986) have found that bottom spraying with organic solvent-based coating results in a higher degree of release retardation than does top spraying. Porter and D'Andrea (1985) have also reported a greater retarding effect on the release after bottom spraying. These differences in coating efficiency have been ascribed primarily to drying of the spray droplets before they hit the substrate, resulting in loss of coating material and film formation that is not optimal (Mehta et al., 1986; Jones, 1988; Li et al., 1989; Holm et al., 1991). However, thus far, the quality of membranes has been assessed theoretically and via examination by scanning electron microscopy.

* Corresponding author.

SSDI 0378-5173(94)00095-M

The purpose of this paper was to examine more closely the differences in physical characteristics of membranes formed by top and bottom spray coating, respectively. Furthermore, the aim was to identify the characteristic(s) responsible for the superior coating efficiency of concurrent coating.

2. Experimental

2.1. Materials

KCl crystals (size 400–900 μm; Klinge Chemicals), ethylcellulose (Ethocel standard 100 mPa s, premium; Dow Chemical Co.), acetyl tributyl citrate (Citroflex A 4, Pfizer), colloidal anhydrous silica (Aerosil 200, Degussa), solid paraffin (ter-Hell Paraffin), and isopropyl alcohol (BP Chemicals) were obtained from the indicated sources.

2.2. Equipment

2.2.1. Coating equipment, laboratory scale

Two fluid-bed systems were used for the application of coating to the KCl crystals. The top-spray unit was a WSG 5 and the bottom-spray unit a GPCG 3 unit with one Wurster partition.

2.2.2. Coating equipment, production scale

Additional production scale trials were performed with both top and bottom spraying. The top-spray unit was a WSG 200 and the bottom-spray unit a GPCG 200/32 inch with three Wurster partitions. The supplier of all units was Glatt GmbH.

2.3. Methods

KCl crystals were coated with a coating solution of the following composition: ethylcellulose 100 mPa s, 4.67%; paraffin, solid, 0.71%; acetyl tributyl citrate, 0.25%; Aerosil 200, 0.07%; isopropyl alcohol, 94.30%. The processing conditions are listed in Table 1.

2.3.1. Methods of characterization

2.3.1.1. Sieve analysis. Sieve analyses were made in a Ro-Tap sieve shaker from Fisher Scientific. All tests were conducted by screening 50 g of crystals for 5 min. An estimate of the specific surface area was based on the assumption of spherical particles. The surface area from each sieve fraction, estimated as the surface area of particles with the midpoint diameters, was summarized.

2.3.1.2. Measurement of specific surface area. The specific surface area of the coated crystals was determined by a permeametry technique in accordance with Eriksson et al. (1990). The apparatus constant was determined by means of reference glass spheres having diameters of 0.7–1.0 mm with a known specific surface area.

2.3.1.3. Determination of dissolution. The release of KCl from the coated crystals was determined

Table 1
Coating conditions

	Laboratory scale		Production scale	
	WSG 5	GPCG 3	WSG 200	GPCG 200/32 inch
Material (kg)	8.0	3.0	300	300
Nozzle position/number of nozzles	top	bottom	top/one 3-head	bottom/three
Spray pressure (bar)	3	3	4.2	2.0
Processing air flow (m^3/h)	180–200	80–100	1500–2000	2000
Liquid flow rate (g/min)	60– 70	28– 35	540– 560	620–660
Coating liquid temperature (°C)	60– 70	60– 70	60– 70	60– 70
Inlet air temperature (°C)	78– 82	70– 75	74– 76	74– 76
Product temperature (°C)	50– 55	55– 60	60	60

by a modified rotating bottle method (Baggesen et al., 1981). The amount of KCl released was detected by means of a potassium-selective electrode.

2.3.1.4. Weibull expression of release curves. The release profiles were described using the Weibull expression:

$$R(t) = 1 - \exp\left[-(t/\tau)^{\beta}\right]$$

where $R(t)$ is the fraction of dissolved substance at time t, τ denotes the time when 63.2% has been dissolved, and β represents the shape of the curve (Christensen et al., 1980).

2.3.1.5. Quantification of coating dry matter applied. 10 g of coated crystals were ground in a Moulinex mill, ensuring that any loss during grinding was less than 1.0%. The powder was suspended in 300 ml of water and placed in the dissolution apparatus for 5 days. The undissolved powder in the bottles was filtered out, rinsed, dried to constant weight and weighed. The powder was transferred to a bottle of 300 ml of water again and placed in the dissolution apparatus for at least 3 days. Subsequently, any residual KCl in the liquid was determined using a potassium-selective electrode. The quantity of coating dry matter was calculated as the quantity of undissolved powder corrected for any undissolved KCl, and the results were stated as % (w/w) of uncoated crystals. All determinations of the quantity of film coating applied were carried out with $n = 5$.

2.3.1.6. Measurement of film thickness. The thickness of the film coating was measured in a transmission light microscope (Leica, Laborlux 5) in a drop of turpentine. At a suitable intensity of light the film coating can be distinguished from the crystal. The thickness of the film coating was measured at three to six points on each of more than 25 crystals. The crystals were chosen randomly.

2.3.1.7. Measurement of film porosity. The porosity of the coated crystals was measured by a pycnometrical technique the principle of which has been described by Strickland et al. (1956). A surface tension of mercury of 0.480 N m^{-1} and a contact angle towards the film coating of 130° were assumed. The porosity, ε was estimated on the basis of an intrusion pressure of 400 mmHg, corresponding to a minimum pore diameter of intrusion of approx. 25 μm. Scanning electron microscopy confirmed that the pores were in general below 25 μm in diameter. The density of the coated crystals, ρ_p, was determined by means of a gas pycnometer (Micrometritics Accu. Pyc. 1330) using helium.

The measured porosity of the coated crystals was recalculated to represent the porosity of the film coating, ε_f, assuming that the KCl crystals are non-porous:

$$\varepsilon_f = \varepsilon/(V_f + \varepsilon)$$

where

$$V_f = \rho_p W/\rho_f$$

W being the amount (w/w) of film coating relative to the KCl crystal, and ρ_f denoting the density of the constituents of the film coating.

2.3.1.8. Pore size distribution. The pore size distribution of the film coating was estimated by a mercury intrusion method (Micrometritics Autopore 2, 9215). The evacuation pressure was 50 μmHg, and the intrusion pressure of the mercury was varied stepwise in the range from 15.9 to 61 000 lb/inch^2. Only pores above 0.1 μm were considered, since the high intrusion pressure of mercury needed for measuring smaller pores may damage the film.

2.3.1.9. Scanning electron microscopy. Three to five coated crystals were embedded in a matrix of epoxy (Araldit®) at the bottom of a gelatine capsule. A cross-section of the crystal was made by means of a microtome, and the sectioned film coating was coated with gold and examined by scanning electron microscopy. The surface structure of the coated crystals was examined by the same technique.

3. Results and discussion

In Fig. 1 the dissolution profiles of coated KCl from five laboratory scale batches with 5.0% ($n = 2$), 6.0% ($n = 2$), and 7.0% ($n = 1$) coating dry matter applied by top spraying are compared with three batches with 6.0% applied by bottom spraying. Fig. 2 shows similar dissolution profiles for two batches coated on a production scale, one batch by the top-spray method and another by bottom spraying. The different amounts of coating dry matter were in this case achieved by sampling during coating of the two batches. Table 2 summarizes the statistical assessment of these batches. The τ values for the laboratory and production scale products suggest that bottom spraying results in 2.6–2.8-times as efficient retardation of the release as does top spraying. This is consistent with the findings of Porter and D'Andrea (1985) and Mehta et al. (1986). For the shape parameter, β (Table 2), there is no difference between top and bottom spraying. In our experience this indicates a similar release mechanism for crystals coated by the two methods.

The observed difference in crystal release retardation can be ascribed to differences in one or more of the following product characteristics: (i) the thickness of the film; (ii) the estimated specific surface area of the coated crystals; (iii) the permeability of the film.

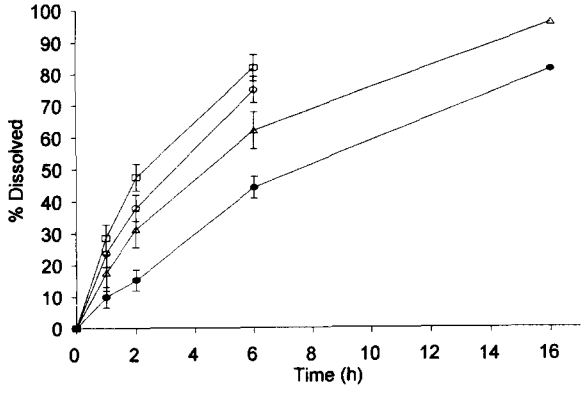

Fig. 1. Dissolution profiles for coated crystals. (□, ○, △) 5.0, 6.0 and 7.0% coating applied on laboratory scale by top spraying; (●) 6.0% coating applied on laboratory scale by bottom spraying. 95% confidence intervals are shown.

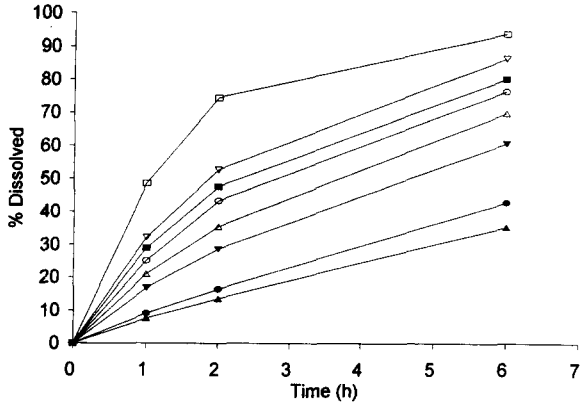

Fig. 2. Dissolution profiles for coated crystals. (□, ▽, ○, △) 4.0, 5.0, 6.0 and 7.0% coating applied on production scale by top spraying; (■, ▼, ●, ▲) 4.0, 5.0, 6.0 and 7.0% coating applied on production scale by bottom spraying.

3.1. Discussion of characteristics

The film thickness for crystals with 6.0% coating dry matter applied on a laboratory scale was 11.5 ± 2.7 μm for top spraying (172 determinations on 28 crystals) vs 13.3 ± 3.3 μm for bottom spraying (259 determinations on 44 crystals). This difference is significant ($p < 0.01$, Student's t-test) although small (16% increase). This is consistent with the findings of Mehta et al. (1986).

The amount of coating dry matter of the nominal 6% applied to these crystals was $5.34 \pm 0.13\%$ ($n = 10$) for top spraying vs $5.70 \pm 0.10\%$ ($n = 15$) for bottom spraying. Bottom spraying thus resulted in a significant ($p < 0.001$, Student's t-test) but small increase (7%) in coating dry matter applied. Li et al. (1989) also found that a larger quantity of coating had been applied after bottom spraying.

Therefore, it can be concluded on the basis of measurements of film thickness and quantification of coating dry matter that bottom spraying results in a larger quantity of dry matter applied than top spraying. However, this increase of approx. 7% and the resulting increase in average film thickness of approx. 16% cannot alone explain the observed increase in τ by a factor of 2.6–2.8. This is clearly demonstrated by the fact that the release after bottom spraying with 6.0% coating dry matter was considerably slower than

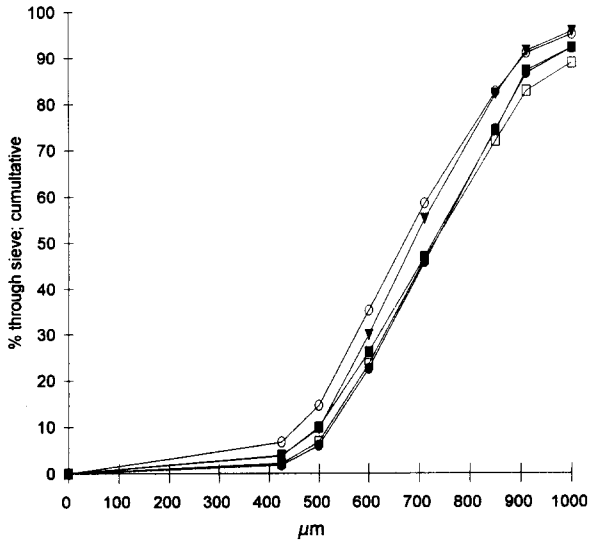

Fig. 3. Sieve analysis of coated crystals with 6.0% coating. (○, □) Coating on laboratory scale by top spraying; (●, ■, ▼) coating on laboratory scale by bottom spraying.

that after top spraying with 7% coating dry matter, although the 7% top sprayed film had a thickness of 13.7 ± 3.5 μm (60 determinations on 13 crystals), and $6.46 \pm 0.21\%$ ($n = 5$) dry matter had been applied.

The specific surface area is a function of the mean particle size, the particle size distribution, and the particle shape. The results of sieve analysis are demonstrated in Fig. 3. The specific surface area by sieve analysis for top spraying with 6% coating dry matter was estimated at $\bar{x} = 47.5 \pm 2.81$ cm^2 g^{-1} ($n = 2$), and for bottom spraying with 6% coating at $\bar{x} = 47.1 \pm 1.26$ cm^2 g^{-1} ($n = 3$). These results show no difference between top and bottom spraying. Therefore, the differences in release retardation observed for crystals after top and bottom spraying cannot be ascribed to changes in specific surface area caused by agglomeration or attrition of the coated crystals.

However, the specific surface area determined by gas permeametry was significantly ($p < 0.02$, Student's t-test) larger for crystals coated by top spraying (119.4 ± 3.4 cm^{-1}, $n = 5$) as compared to bottom spray crystals (110.7 ± 5.0 cm^{-1}, $n = 3$). Since the specific surface area by sieve analysis showed no difference, the difference in surface area observed via gas permeametry could be due to differences in the surface structure of the coatings. On performing scanning electron microscopy, a rougher surface could actually be observed on crystals from top-spray coating. These observations are in agreement with that of Mehta and Jones (1985).

The rougher surface after top spraying would alone cause a slightly increased release rate, even though the average film thickness was unchanged, as a comparatively faster release would be achieved through a thinner layer. However, extremely large differences in film thickness would be required if they were to be the cause of the observed differences in τ. Since there was no difference between the top and bottom spray

Table 2
Statistical evaluation by ANOVA of dissolution results from crystals coated with 6.0% coating

Scale	Equipment	Number of batches	% dissolved of label claim averages ($n = 3$)					
			1 h	2 h	6 h	β	τ	r
Laboratory	top	2	23.8	38.2	75.0	0.92	4.30	0.999
	bottom	3	10.0	15.3	44.3	0.98	11.0	0.991
Production	top	1	25.1	43.3	76.6	0.90	3.90	0.999
	bottom	1	9.11	16.5	43.0	0.99	10.9	1.000
Standard error			2.4	3.2	3.9	0.065	0.82	
Statistical analysis								
Scale			$p <$ n.s.	n.s.	n.s.	n.s.	n.s.	
Equipment			$p < 0.01$	0.001	0.001	n.s.	0.001	
Scale × equipment			$p <$ n.s.	n.s.	n.s.	n.s.	n.s.	

n.s., not significant, i.e., $p > 0.05$; r, correlation coefficient.

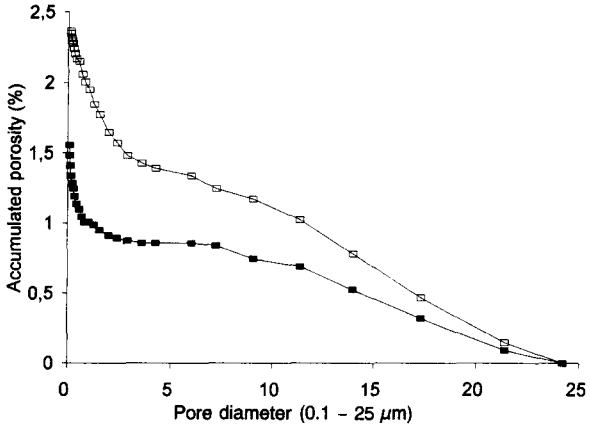

Fig. 4. Porosity accumulated from a diameter of 25 μm to the calculated pore diameter. The porosity is stated in % of the coated crystals. (□) 6.0% applied by top spraying, laboratory scale; (■) 6.0% applied by bottom spraying, laboratory scale.

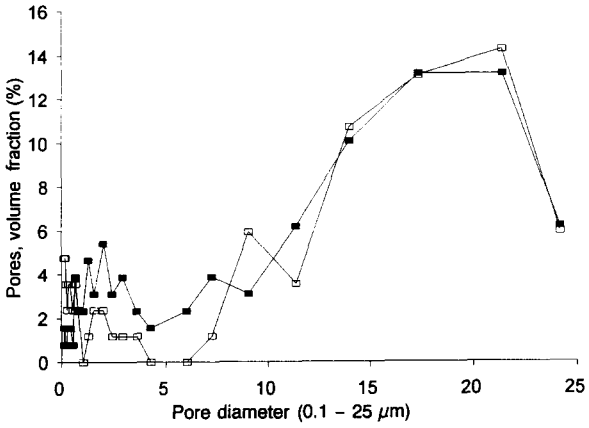

Fig. 5. Pore volume fraction of coated crystals as a function of pore diameter. (□) 6,0% applied by top spraying, laboratory scale; (■) 6.0% applied by bottom spraying, laboratory scale.

films as far as variation in the measured film thickness is concerned, the rougher surface after top spraying cannot explain the differences in retardation.

The porosity values of the coated crystals showed that top spraying resulted in a film coating with a significantly ($p < 0.005$, Student's t-test) higher average porosity ($29.9 \pm 4.6\%$, $n = 6$) compared to bottom spraying ($18.1 \pm 6.4\%$, $n =$

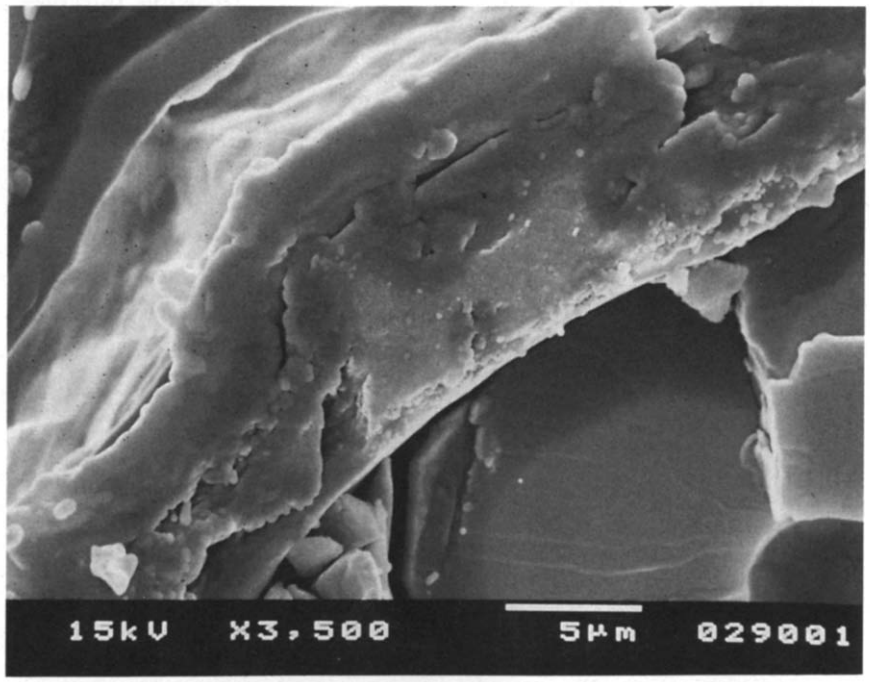

Fig. 6. Cross-section of coating applied by top spraying (laboratory scale). Magnification, 3500 ×.

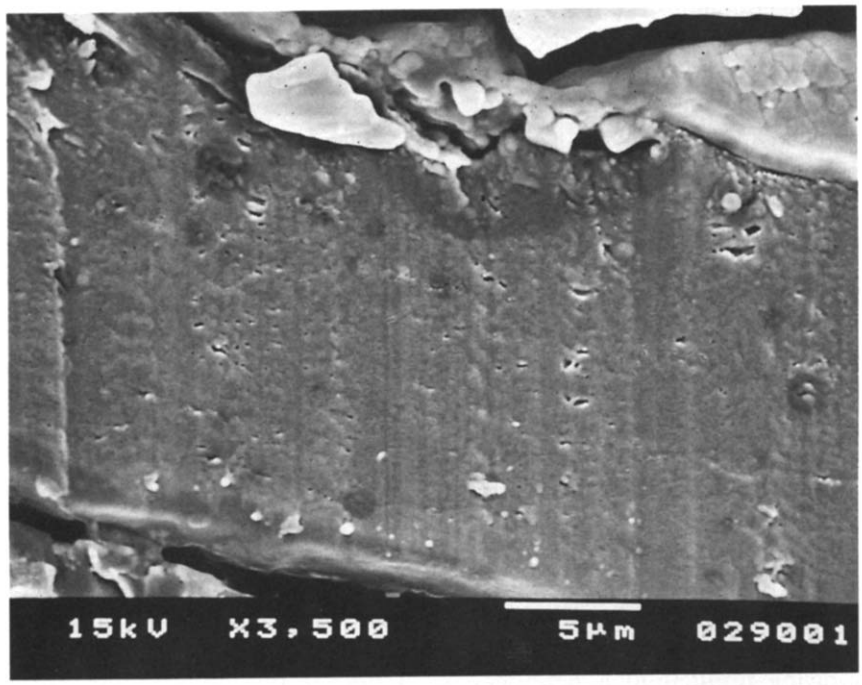

Fig. 7. Cross-section of coating applied by bottom spraying (laboratory scale). Magnification, 3500 × .

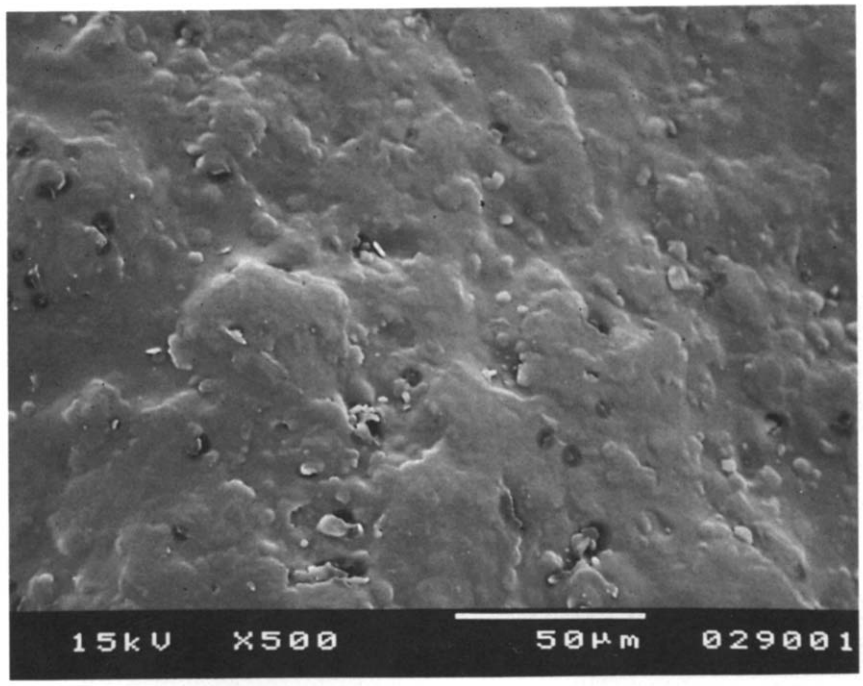

Fig. 8. Surface structure of coating applied by top spraying (laboratory scale). Magnification, 500 × .

6). The same pattern is demonstrated in Fig. 4 showing the accumulated porosity from the pore size distribution measurement. However, even though the porosity of film coatings is dependent on the spraying principle, there was practically no difference in pore size distribution (Fig. 5).

The difference in porosity corresponds to an increase in pore volume by approx. 60% after top spraying. Assuming that the transport of potassium chloride takes place in pores, this difference in pore volume can explain much of the difference in τ observed after top and bottom spraying. As increased porosity of the film after top spraying is the main difference, it is conceivable that the release mechanism after top and bottom spraying is the same, as also indicated by the β values of top and bottom spraying.

The observations made by scanning electron microscopy of approx. 50 cross-sections of film coatings from top and bottom spraying showed a clear difference in structure as exemplified in Fig. 6 and 7. Top spraying resulted in a heterogeneous, porous film structure with areas of cracks and spray-dried spherical particles. In contrast, the coatings after bottom spraying were porous but homogeneous, and fewer cracks were observed. Furthermore, no spray-dried particles were observed.

The observations were confirmed by scanning electron microscopy of the surface characteristics of the coatings (Fig. 8 and 9). Spray-dried particles were observed after top spraying, whereas the film coating after bottom spraying was in general more homogeneous. Holes up to a diameter of approx. 25 μm appeared in the surface of the coating for both coating techniques. The higher porosity after top spraying is reflected in the surface roughness as observed under the scanning electron microscope. The larger number of dried particles in top spraying can be ascribed to a greater number of droplets having lost so much solvent before they hit the substrate, that satisfactory spreading and contact with the underlying film layer are not achieved. Some of the droplets lose so much solvent that they do not adhere to the substrate but leave the equipment. As shown by the quantification of coating dry matter applied, this loss was doubled in connec-

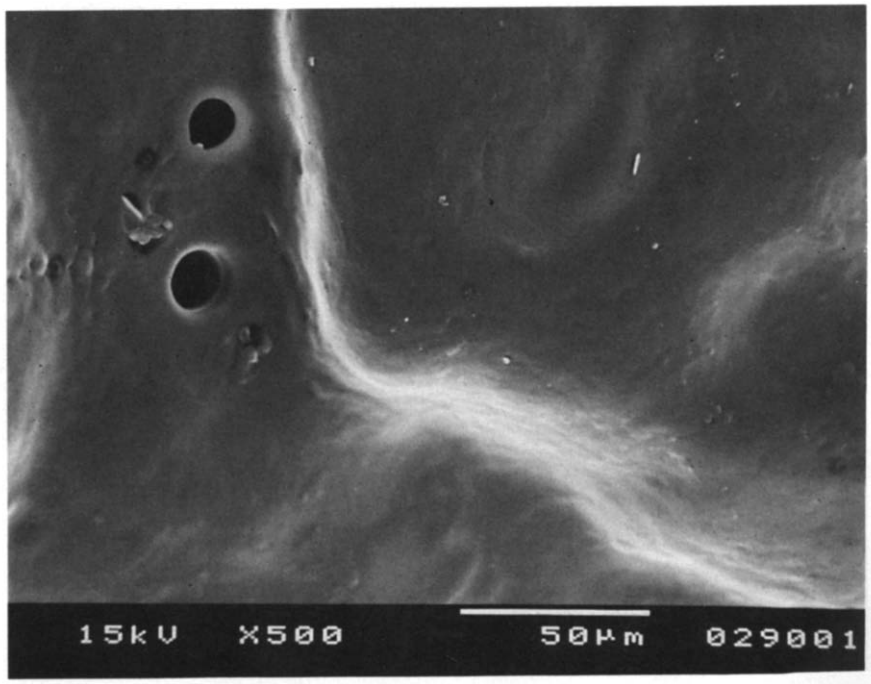

Fig. 9. Surface structure of coating applied by bottom spraying (laboratory scale). Magnification, 500 ×.

tion with top spraying (11% lost material) as compared with bottom spraying (5% lost material). The loss of material out of the equipment is, however, of less importance for the release retardation than the change in membrane porosity caused by poor spreading of droplets.

The difference between top and bottom spraying is considered primarily to be caused by variation in the distance between nozzle and crystals. This distance, which should be minimized to reduce evaporation of solvent from the droplets, will vary from particle to particle to a much larger extent in a top-spray than in a bottom-spray system. Furthermore, the average distance from nozzle to substrate will be greater in top-spray than in bottom-spray equipment. The distance has also been described by Jones (1988) as a very important parameter.

Another difference is that, unlike top-spray coating, particles and coating liquid travel in almost the same direction in concurrent coating. Therefore, it is conceivable that the spreading of the film solution is more gentle and thus homogeneous. Conversely, countercurrent coating involves a high relative speed of the film droplets towards the particles, giving rise to excessive spreading of the droplet.

4. Conclusion

A comparison of organic solvent-based coating in top-spray equipment and bottom-spray equipment with Wurster partition(s) has shown that bottom spraying results in more efficient retardation. This difference can primarily be ascribed to a difference in the porosity of the membrane applied and consequently to a difference in the barrier properties of the membrane. The varying degrees of retardation cannot be explained by differences in loss of coating material in the two types of equipment. Nor can variations in film thickness or differences in attrition or agglomeration during the coating process explain the difference in retardation.

Evaluation of film qualities by scanning electron microscopy alone is not sufficient to explain differences in retardation. It must be supported by quantification of the relevant physical characteristics of the film to give a better understanding of the differences that can be observed under the scanning electron microscope and to identify the differences important for the retardation.

Acknowledgements

We would like to thank Roger Schütz-Trapp of Glatt GmbH and Charles M. Hansen of the Force Institutes for technical assistance, and Mette Lykke Møller and Jette Brammer for support with laboratory work.

References

Baggesen, S., Bechgaard, H. and Schmidt, K., Content and dissolution uniformity testing of controlled release products. The Repro-Dose® quality control procedure. *Pharm. Acta Helv.*, 56 (1981) 85–92.

Christensen, F.N., Hansen, F.Y. and Bechgaard, H., Physical interpretation of parameters in the Rosin-Rammler-Sperling-Weibull distribution for drug release from controlled release dosage forms. *J. Pharm. Pharmacol.*, 32 (1980) 580–582.

Eriksson, M., Nyström, C. and Alderborn, G., Evaluation of a permeametry technique for surface area measurements of coarse particulate materials. *Int. J. Pharm.*, 63 (1990) 189–199.

Holm, P., Holm, J. and Lång, P.O., A comparison of two fluid bed systems. Enteric coating of pellets. *Acta Pharm. Nord.*, 3 (1991) 235–241.

Jones, D.M., Air suspension coating. In Swarbrick, J. and Boyland, J.C. (Eds), *Encyclopedia of Pharmaceutical Technology*, Dekker, New York, Vol. 1, 1988, pp. 189–216.

Li, S.P., Feld, K.M. and Kowarski, C.R., Preparation of a controlled release drug delivery system of indomethacin: Effect of process equipment, particle size of indomethacin, and size of the nonpareil seeds. *Drug Dev. Ind. Pharm.*, 15 (1989) 1137–1159.

Mehta, A.M. and Jones, D.M., Coated pellets under the microscope. *Pharm. Technol.*, 9 (1985) 52–60.

Mehta, A.M., Valazza, M.J. and Abele, S.E., Evaluation of fluid-bed processing for enteric coating systems. *Pharm. Technol.*, 10 (1986) 46–56.

Porter, S.C. and D'Andrea, L.F., The effect of choice of process on drug release from non-pareils film coated with ethylcellulose. *Paper presented at the 12th International Symposium on Controlled Release of Bioactive Materials*, Geneva, July, 1985, pp. 41–42.

Strickland, W.A., Jr, Busse, L.W. and Higuchi, T., The physics of tablet compression: XI. *J. Am. Pharm. Assoc.*, 45 (1956) 482–486.